Pergamon

0038-1101(94)00258-4

Solid-State Electronics Vol. 38, No. 7, pp. 1313–1319, 1995

0038-1101/95 $9.50 + 0.00

EVOLUTION OF DISLOCATION LOOPS IN SILICON IN AN INERT AMBIENT—II

S. CHAUDHRY[1], J. LIU[2], K. S. JONES[2] and M. E. LAW[1]

[1]Department of Electrical Engineering, 214 A Rhines Hall and [2]Department of Materials Science and Engineering, University of Florida, Gainesville, FL 32611, U.S.A.

(Received 18 October 1994)

Abstract—A plan-view TEM study of the distribution, geometry and time-dependent anneal behavior of type-II dislocation loops induced by $1 \times 10^{15}/cm^2$, 50 keV Si^+ implantation into silicon was presented in Part I of this paper. A point-defect based model representing loop-to-loop interactions (Ostwald-ripening) during annealing is developed. The variation in the size and distribution of the loops as a function of anneal time and temperature is correctly simulated as part of this modeling exercise. Other quantities of interest, such as the average radii of the loop distribution are extracted from the model and directly compared with experimental values.

1. INTRODUCTION

The use of high-dose ion-implantation to obtain heavily doped regions in silicon such as the source and drain of a MOSFET has gained immense popularity in recent years due to the inherent controllability of the implanted profile. However the damage created in the substrate by the process strongly affects dopant redistribution during later anneals. During annealing solid-phase epitaxial regrowth of the amorphized region leads to the formation of end-of-range dislocation loops at the amorphous/crystalline (a/c) interface. It has been shown that the end-of-range dislocation loops affect the distribution of point defects by the absorption of interstitials or emission of vacancies at their core boundary during growth, and by the reverse process during shrinkage[1,2].

Earlier work[3–6] established theoretical models for a single circular dislocation loop and its interaction with point defects. Bullough *et al.*[4] used Bastecka and Kroupa's[5] stress field solution to predict the migration of a single interstitial atom around a single dislocation loop. Borucki[6] proposed a model for the growth and shrinkage of a single dislocation loop due to the capture and emission of point defects, and simulated the point defect variation from an assumed initial high super-saturation around a periodic array of the loops in a three-dimensional numerical solver of diffusion equations. Park and Law[1] developed a statistically based model for loop-growth in an oxidizing ambient, where the interstitials injected from the growing oxide contribute to the growth of the large loops. Pressure effects from the loops were incorporated into the point-defect equations. Part I of this paper demonstrated that in an inert ambient loop-growth kinetics are mainly governed loop-to-loop interactions, with the large loops growing at the expense of smaller ones: (Ostwald ripening). This work quantitatively analyzes the size and density distribution of the loops as a function of anneal time and temperature.

2. EXPERIMENTAL DETAILS

Czochralski single crystal wafers [⟨100⟩ orientation, boron doped ($1 \sim 100\,\Omega$ cm), $600 \sim 650\,\mu$m thick] were used as the starting material. Si^+ was then implanted at 50 keV and a dose of $1 \times 10^{15}/cm^2$ to produce type-II dislocation loops[7]. After implantation, the whole wafer was capped with 6000 Å of SiO_2 before the annealing process to limit any oxidation in the inert ambient. The wafers were then cut into four parts and were annealed in a nitrogen ambient at 700, 800, 900 and 1000°C for times ranging from 15 min to 16 h. The capped oxide for all samples was removed by HF before mechanical etching and jet-etching. For detailed methods of measuring the total loop density, the average loop size, the loop distribution and the interstitials bound by loops, please refer to Part I of this work.

3. EXPERIMENTAL RESULTS

The loop distribution $N(r)$ versus loop radius r is shown for the various anneal conditions is shown in Figs 1–4. $N(r)$ represents the loop density at radius r. A shift in the loop distribution towards a larger radius is observed with increasing time for each temperature. The velocity of this movement is smaller for the low temperature anneals. Again this tendency is the result of the loop coarsening process. It should be pointed out that because $N(r)$ is proportional to r^2, the plot for large r is expected to show considerable scatter, particularly when the number of loops

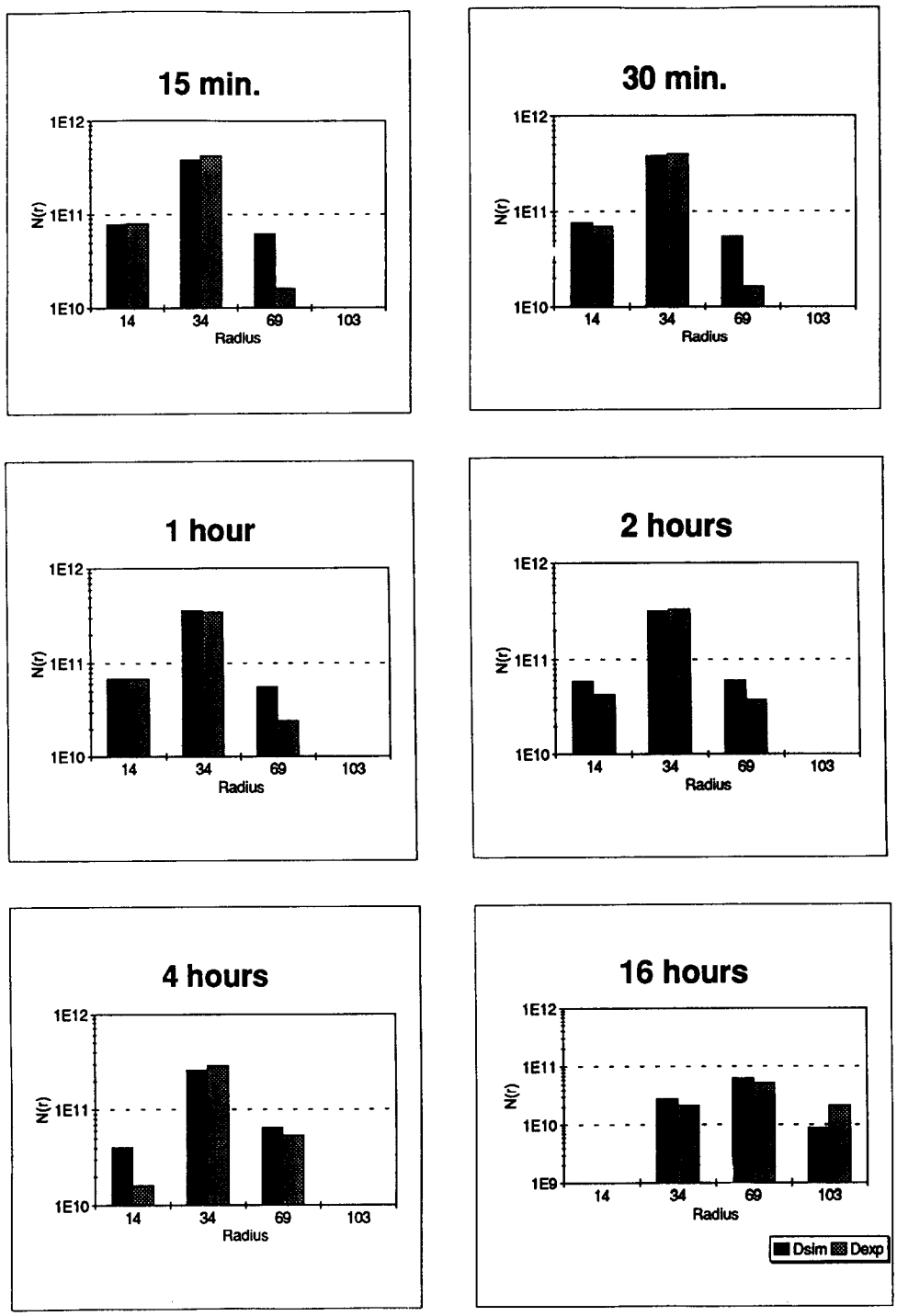

Fig. 1. Size spectra of loops as a function of loop radius after annealing in N_2 at 700°C for anneal times ranging from 15 min to 16 h. The radius is in angstroms and the density is cm^{-2}.

counted is relatively small, as in the case of the 1000°C anneal. If the temperature is kept constant, the loop size increases with anneal time, although at low temperatures (700, 800°C) this movement appears to be much slower than that at high temperatures (900, 1000°C). The total loop density decreases for increasing anneal times, causing the density of interstitials bounded by the loops stay constant for low temperatures and decrease with annealing for high temperatures. For annealing times greater than 2 h at 1000°C stacking faults are formed.

The average loop radius is measured for each annealing condition. Figure 5 shows the average loop radius versus annealing time at different temperatures. An increase in average loop radius was observed with increasing time, though it is quite slow for

low temperatures. At the early stage of the 700°C anneal, the loops are quite small, but after 4 h of annealing, they are well developed. It is also apparent that as temperature increases, the average loop radius increases, which means more of the implantation induced supersaturated interstitials move to the dislocation loops as the temperature goes up. The average loop radius for 1000°C anneal is much larger than that of the other temperatures.

The total loop densities are shown in Fig. 6. A decrease in the densities is observed with increasing anneal time, and if the time is kept constant, the density is found to decrease with an increase in temperature. This is the result of the loop coarsening

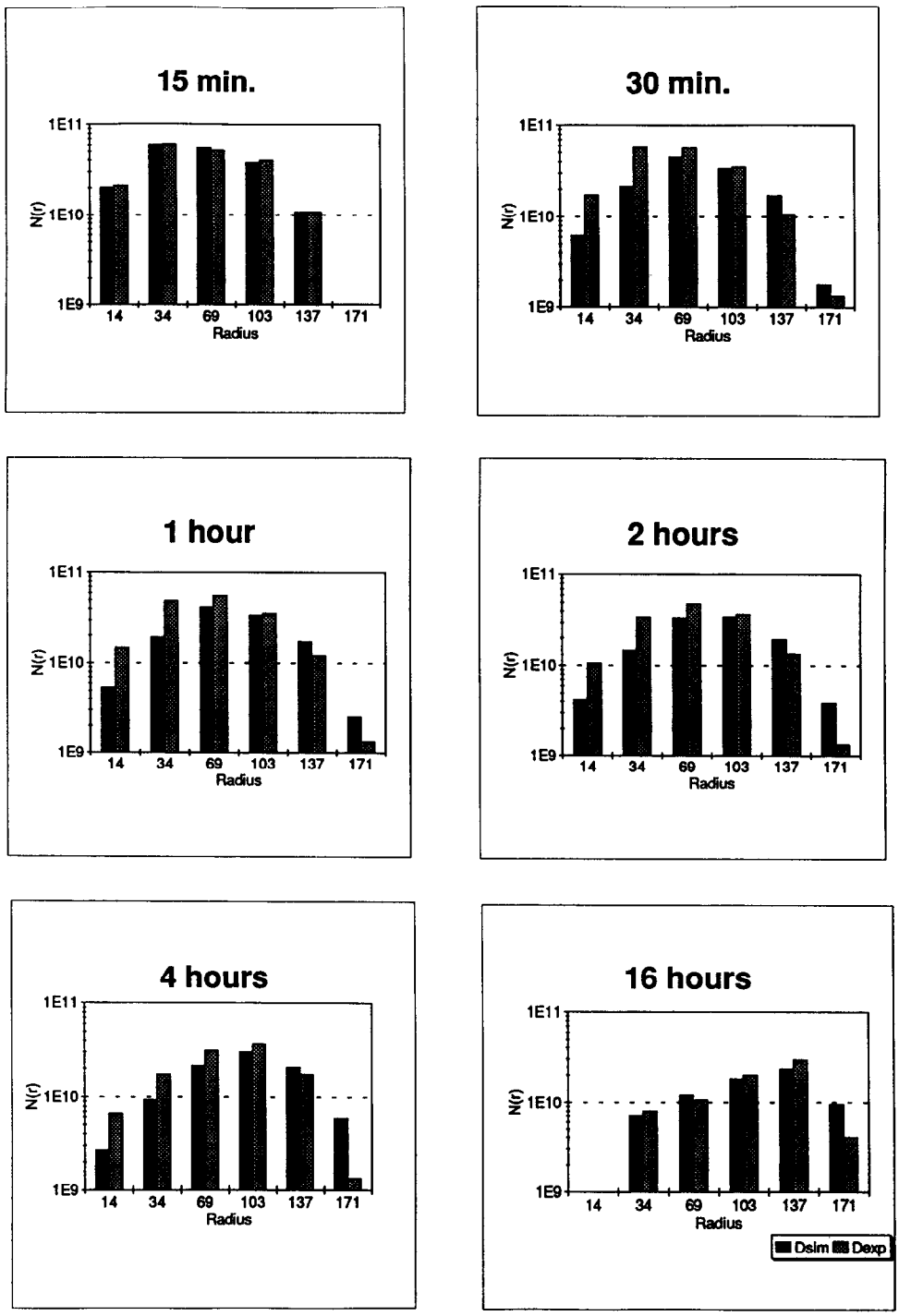

Fig. 2. Size spectra of loops as a function of loop radius after annealing in N_2 at 800°C for anneal times ranging from 15 min to 16 h. The radius is in angstroms and the density is cm^{-2}.

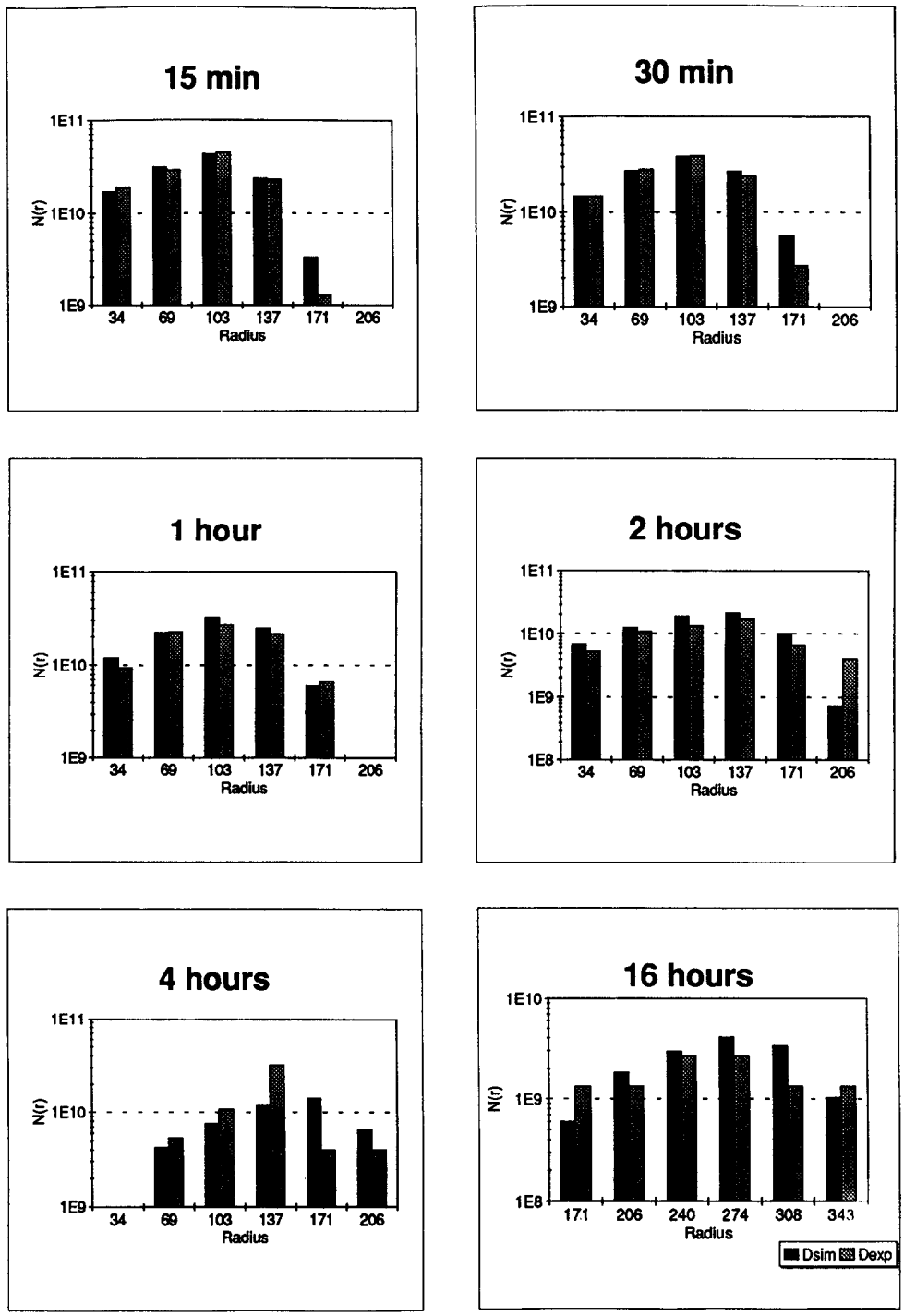

Fig. 3. Size spectra of loops as a function of loop radius after annealing in N_2 at 900°C for anneal times ranging from 15 min to 16 h. The radius is in angstroms and the density is cm^{-2}.

process, during which the larger loops grow at the expense of smaller ones.

Loops begin their dissolution right after the 1000°C anneal. For the 700 and 800°C anneals, the loops remain in the coarsening regime and the densities of interstitials bound by the loops remain fairly constant (Fig. 4 in Part I). For the 900°C anneal, the density of the captured interstitials decreases with increasing time, however the larger loops do continue to grow, while the smaller loops continue to shrink and eventually vanish.

4. MODELING

As can be seen from the experimental data in Figs 1–4, the loops distribution can be modeled in the

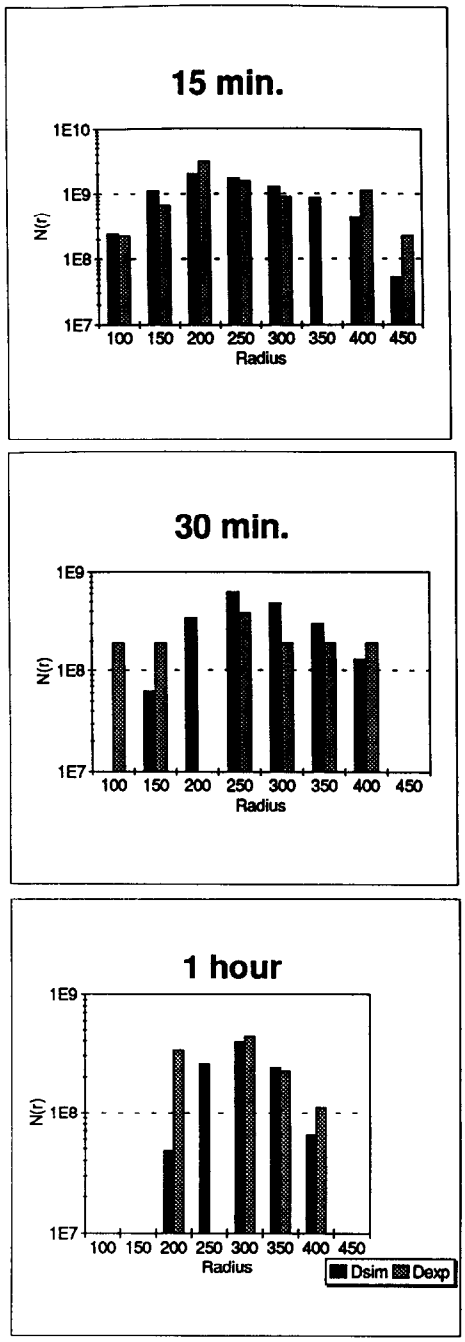

Fig. 4. Size spectra of loops as a function of loop radius after annealing in N_2 at 1000°C for anneal times ranging from 15 min to 2 h. The radius is in angstroms and the density is cm^{-2}.

form of an asymmetrical triangular distribution function. Such a model has been developed by Park and Law[1]. It assumes circular loops distributed on a plane interconnecting their centers. The orientation of the loops was assumed periodic in two perpendicular directions. The radius and density are assumed to follow an asymmetric distribution function. Each set of data is characterized by its minimum radius (R_{min}), its peak radius (R_p), where the density of the loops is

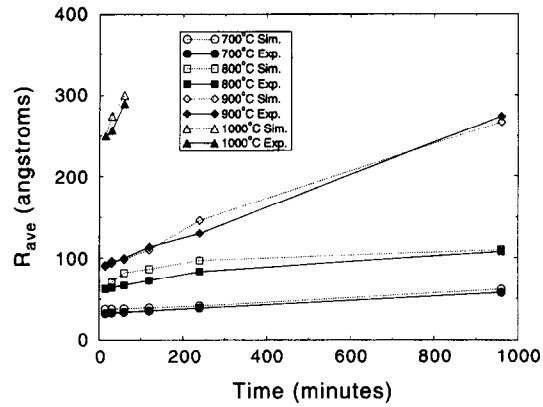

Fig. 5. Variation in average loop radius as a function of anneal time at different temperatures.

a maximum ($=D_p$), and the maximum radius of the distribution (R_{max}). The total density of the distribution is represented by D_{all}. The unnormalized probability distribution function $f_d(R)$ is then represented as:

$$f_d(R) = \frac{2D_{all}(R - R_{min})}{(R_{max} - R_{min})(R_p - R_{min})}$$

when $R_{min} < R < R_p$ (1)

$$f_d(R) = \frac{2D_{all}(R_{max} - R)}{(R_{max} - R_{min})(R_{max} - R_p)}$$

when $R_p < R < R_{max}$. (2)

The density at a particular radius $D(R)$, is then given as:

$$D(R) = \int_{R-\frac{\Delta R}{2}}^{R+\frac{\Delta R}{2}} f_d(R')\,dR' = f_d(R)\Delta R \quad (3)$$

The density D_p of the majority loops with radius R_p and its relation with the total density D_{all} can be expressed by using eqns (1), (2), and (3):

$$D_p = f_d(R_p)\Delta R = \frac{2D_{all}\Delta R}{R_{max} - R_{min}} = \frac{2D_{all}}{m}, \quad (4)$$

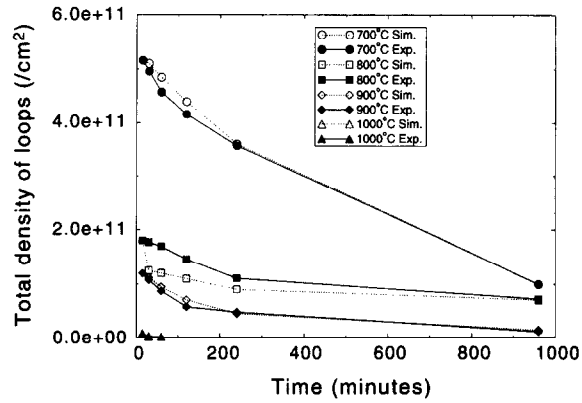

Fig. 6. Variation in total loop density as a function anneal time at different temperatures.

where m is defined to be $(R_{max} - R_{min})/\Delta R \equiv 2D_{all}/D_p$. The average radius for a given distribution is derived in [1] as:

$$R_{ave} = \tfrac{1}{3}(R_{min} + R_p + R_{max}). \quad (5)$$

The model is described in detail in Ref. [1]. The model is extended and suitably modified to account for loop-to-loop interactions as was observed in the experimental data. Growth and shrinkage of the dislocation loops are modeled in terms of their reaction with point defects at the loop layer boundaries. The boundary conditions are given by the reaction rates of dislocation loops and the point defect formation energy change due to loop growth or shrinkage. The interstitial continuity equation in the presence of dislocation loops is derived in [1], and is used in the current model as well.

The annealing behavior of type-II dislocation loops follows the Ostwald ripening process of loop-coarsening governed by a bulk-diffusion phenomenon[8, Part I this work]. The effective local equilibrium concentration of interstitials is at the loop layer boundary, C_{Ib} is given in [6,9] as:

$$C_{Ib} = g_{bc} C^*_{I(P)} \exp(-\Delta E_f/kT) \quad (6)$$

$$C_{Vb} = g_{bc}^{-1} C^*_{V(P)} \exp(\Delta E_f/kT), \quad (7)$$

where g_{bc} is a geometric factor ($\cong 0.3$), $C^*_{I(P)}$ is the pressure dependent concentration of interstitials, k is the boltzman's constant and T is the absolute temperature. ΔE_f is the change in defect formation energy due to the self-force of a dislocation loop during the emission and absorption process at its edge and is given in [3] as:

$$\Delta E_f = -\frac{\mu \mathbf{b} \Omega}{4\pi(1-v)R}\left[\ln\left(\frac{8R}{r_c}\right) - \frac{2v-1}{4v-4}\right], \quad (8)$$

where μ is the shear modulus, $\mathbf{b}$ is the magnitude of the Burgers vector of the loop, Ω is the atomic volume of silicon, r_c is the core (torus) radius of the loop, v is the Poisson's ratio, and R is the radius of the dislocation loop. According to eqn (6), the concentration of self-interstitials at the periphery of a dislocation loop of radius r_1 is lower than that at the periphery of a loop of radius r_2, when $r_1 > r_2$. Therefore, a gradient in the concentration of self-interstitials will be established between dislocation loops with different radii. This concentration gradient induces a self-interstitial flux from small loops to larger ones. As a result larger loops grow and smaller loops shrink until they eventually vanish. This constitutes the dislocation loop coarsening process. A schematic diagram to illustrate the silicon self-interstitial concentration gradient established due to the size difference of dislocation loops is shown in Fig. 7.

The radii and the density of the majority-sized loops (or the unit distance L_p between the loops) can be correlated with the number of silicon atoms bound by the dislocation loops per unit area ($n(R_p)$), consid-

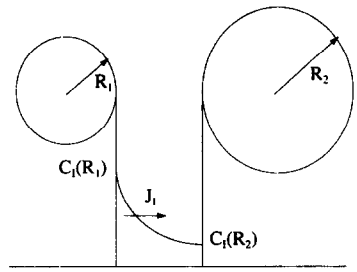

Fig. 7. Schematic diagram to illustrate the Si self-interstitial concentration gradient established due to the size difference of the dislocation loops.

ering that the density of majority size loops D_p is equal to $0.5L_p^{-2}$:

$$n(R_p) = (0.5 \cdot \pi n_a R_p^2)/L_p^2, \quad (9)$$

where n_a is the atomic density of Si atoms on the (111) plane ($= 1.5 \times 10^{15}\,\text{cm}^{-2}$). Now if n, is the density of interstitials bound at radius R of the ensemble, its time derivative should equal the absorption of interstitials or the emission of vacancies at the loop layer boundaries, i.e.:

$$\left.\frac{\partial n}{\partial t}\right|_{\text{at Radius } R} = \alpha K_{IL}(C_I - C_{Ib}) - \alpha K_{VL}(C_v - C_{Vb})|_{\text{at Radius } R} \quad (10)$$

where α is an effective cross section of the loop layer in the unit of linear length, K_{IL} is the constant of reaction between the interstitials and the dislocation loop collection, K_{VL} is a similar constant for vacancies, $C_{I/V}$ is the concentration of interstitials/vacancies, and $C_{Ib/Vb}$ are defined in eqn (6, 7). It is apparent that during the coarsening process the smaller loops loose Si atoms to the larger ones, thus the quantity in eqn (10) should be positive above a certain value of the radius (R_{crit}), and negative below it, i.e.

$$\frac{\partial n}{\partial t} < 0 \quad \text{for} \quad R < R_{crit} \quad (11)$$

$$\frac{\partial n}{\partial t} > 0 \quad \text{for} \quad R > R_{crit}. \quad (12)$$

Such results were confirmed using simulations in FLOOPS (Florida Object Oriented Process Simulator). In our model we calculate the net loss of Si atoms at an average size [$=(R_{min} + R_p)/2$] and let this loss of atoms be transferred to the growth of the loops of radius R_p, i.e.:

$$\left.\frac{\partial n}{\partial t}\right|_{R_p} = \left.\frac{\partial n}{\partial t}\right|_{R_{min} + R_p/2}. \quad (13)$$

The relationship between the time derivatives of R_p and n is derived in [1] as:

$$\left.\frac{\partial n}{\partial t}\right|_{R_p} = \left[\frac{\partial n}{\partial R_p} + \frac{\partial n}{\partial L_p}\cdot\frac{dL_p}{dR_p}\right]\left(\frac{\partial R_p}{\partial t}\right), \quad (14)$$

where the first two derivatives on the right are evaluated using eqn (9). Thus eqns (13) and (14) give the time rate of change of the peak radius which is then used to obtain the time rate of change of the other distribution parameters from empirically observed relationships as described by Park and Law[1]. The distribution parameters were extracted at each time step and density histograms $[N(r)]$ were extracted to plot with the experimental data (Figs 1–4). The major parameter in fitting this model to the data is K_{IL}, and is extracted as:

$$K_{IL} = 1.6e7 \exp(-1.01/kT). \quad (15)$$

The model agrees well with experimental data for most anneal conditions. The loop coarsening phenomenon is well modeled for most anneal conditions. For 700°C minor variations exist in the height of the histograms for anneals up to 16 h. The total density (Fig. 6) of the loops agrees well with the experimental values at this temperature. For 800°C the model predicts a slightly higher initial dissolution rate of the loops, which causes small differences in the experimental and simulated bin sizes. Again good agreement is obtained for the 900°C anneals. Variations in bin sizes for the experimental and simulated cases vanish if two adjacent bins are added and plotted together. Such an assumption is valid due to a strong possibility of scatter in the TEM measurements. This also accounts for the differences in the bin sizes at 1000°C, where large scattering is observed in the experimental data. It should be noted that efforts to model the initial distribution of loops by an asymmetric distribution function for the 15 min/1000°C case lead to some errors which are propagated as the simulation progresses. However good agreement for the total density of loops is again obtained at this temperature.

Simulated values for the average radius are plotted along with the experimental values in Fig. 5. As can be seen the model correctly predicts the average value of the radius for most anneal conditions.

5. CONCLUSION

A plan-view TEM study of the evolution of dislocation loops in silicon during annealing has been presented. It has been shown that with increasing anneal time the average size of the loops increases while the total density of distribution decreases. The same effects is observed with increasing temperature if the anneal time is kept a constant. At 1000°C stacking faults are formed beyond 2 h of annealing. The loop evolution is shown to follow the Ostwald-ripening phenomenon with the large loops growing at the expense of smaller ones.

A point defect based model which physically accounts for loop-to-loop interactions is developed from Park and Law's[1] model. It correctly predicts the evolution of loops for most anneal conditions. Constants which define the rate of reaction between the loops and point defects are extracted for the temperature range 700–1000°C.

REFERENCES

1. Heemyong Park, K. S. Jones and M. E. Law, *J. electochem. Soc.* **141,** 759 (1994).
2. R. B. Fair, J. J. Wortman and J. Liu, *J. electochem. Soc.* **131,** 2387 (1984).
3. S. D. Gavazza and D. M. Barnett, *J. Mech. Phys. Solids* **24,** 171 (1976).
4. R. Bullough, J. T. Stanley and J. M. Williams, *Metal Sci. J.* **2,** 93 (1968).
5. J. Bastecka and F. Kroupa, *Czech. J. Phys.* **B14,** 443 (1964).
6. L. Borucki, Paper presented at Workshop on Numerical Modeling of Processes and Device for integrated circuits: NUPAD iV, Seattle, WA (1992).
7. K. S. Jones, S. Prussin and E. R. Weber, *Appl. Phys. A* **45,** 1 (1988).
8. B. L. Eyre and D. M. Maher, *Phil. Mag.*, 767 (1971).
9. J. P. Hirth and J. Lothe, *Theory of Dislocations*, 2nd Edn, pp. 497–516. Wiley, New York (1982).